**Journal of Creativity Student**
http://journal.unnes.ac.id/journals/jcs

# Experimental Analysis of Performance, Fuel Consumption, and Noise in Three Exhaust Configurations of a 145 cm³ Bore-Up Yamaha Jupiter Z

Mahendra Suryo Prabowo[1]*, Kriswanto[2], Abdurrahman[3], Basyirun[4], Ahmad Roziqin[5]

[1-5]*Department of Mechanical Engineering, Universitas Negeri Semarang, Indonesia*

*Corresponding Author: mahendrasurya95@students.unnes.ac.id

**Abstract**
Exhaust-system modification is a creative engineering problem because gains in engine performance can conflict with fuel-use efficiency and acoustic control. This study evaluates three exhaust configurations standard, free-flow, and Hight Performance Low Pollution Muffler (HPLPM) Mod 2 on a 145 cm³ bore-up Yamaha Jupiter Z engine to identify their multi-criteria trade-offs. A laboratory experiment measured torque and brake power using a chassis dynamometer, fuel consumption using a volumetric method, and A-weighted sound pressure level under controlled operating conditions. The free-flow configuration produced the highest maximum torque (13.10 N·m) and brake power (13.10 HP) and showed lower fuel consumption at low-to-medium engine speeds, although consumption increased at high speed. HPLPM Mod 2 consistently provided the strongest acoustic control, with a maximum measured level of 95.55 dB(A), compared with 101.85 dB(A) for the free-flow configuration. These results show that no single exhaust configuration simultaneously optimizes all performance criteria. The study contributes a multi-criteria experimental basis for creative exhaust-system selection: free-flow prioritizes performance, whereas HPLPM Mod 2 offers a more balanced compromise between performance and noise control.

**Keywords:** *biomaterial, Di Elaeocarus ganitrus, ecoprint, falen leaves, sustainable textiles*

## INTRODUCTION

Spark ignition (SI) internal combustion engines remain relevant in two-wheeled vehicles due to their production costs, ease of maintenance, and competitive power-to-weight ratios (Pirrello et al., 2024; Markiewicz, 2024). The development challenges are no longer singular: performance enhancement needs to be considered alongside energy efficiency, emissions, and acoustic comfort (Novella et al., 2024; Wang et al., 2023; Sutisna & Ramadhan, 2025). This condition renders the development of engine supporting components a multi-objective engineering problem, namely seeking configurations that not only yield high output but also fulfill competing operational requirements. Among the components shaping SI engine characteristics, the exhaust system is a design element directly related to combustion gas flow, backpressure, and the gas exchange process (Sutisna & Ramadhan, 2025; Murali et al., 2021).

Changes in these characteristics correlate with volumetric efficiency, torque, power, and fuel consumption (Uzoechi et al., 2025; Khoa & Lim, 2021). Therefore, exhaust optimization serves as an engineering space that enables the exploration of alternative configurations without requiring major modifications to the basic engine construction (Sutisna & Ramadhan, 2025; Choe et al., 2021; Sugiarto et al., 2025). In the context of engineering creativity, the quality of a solution is determined not only by its novelty in form but by the configuration's ability to simultaneously address multiple technical needs. Increasing cylinder capacity through bore-up modifications produces a larger exhaust gas volume compared to standard engines, thereby altering flow conditions within the exhaust system (Sutisna & Ramadhan, 2025; Khoa & Lim, 2021). These alterations can affect backpressure, pressure wave propagation, the scavenging process, as well as torque output, power, fuel consumption, and acoustic characteristics (Uzoechi et al., 2025; Khoa & Lim, 2021). Consequently, an adequate exhaust configuration for a standard engine may not necessarily yield the same compromise when applied to a bore-up engine, thus necessitating direct evaluation under modified engine conditions.

The exhaust system also functions as a noise control device through acoustic attenuation mechanisms in the muffler (Sutisna & Ramadhan, 2025; Huang et al., 2025; Ao et al., 2025). Enhancing attenuation capabilities, however, can be accompanied by an increase in exhaust gas flow resistance, meaning that acoustic and performance objectives do not always align (Sutisna & Ramadhan, 2025; Ao et al., 2025). Thus, the selection of an exhaust configuration is a compromise-based design decision, rather than merely a pursuit of a configuration with maximum power. Previous studies indicate that changes in exhaust flow configurations correlate with volumetric efficiency, torque, and power (Uzoechi et al., 2025; Khoa & Lim, 2021), while changes in the internal geometry of the muffler can enhance acoustic attenuation by increasing transmission loss, with the potential consequence of pressure loss (Huang et al., 2025; Fu et al., 2025). The literature demonstrates that exhaust system optimization fundamentally demands a balance between performance and acoustic characteristics (Sutisna & Ramadhan, 2025; Murali et al., 2021). This tension between criteria serves as the basis for evaluating several alternative configurations within a single experiment, allowing design decisions to be made based on multi-parameter evidence.

Although the influence of the exhaust system on both performance and acoustics has been extensively studied, some research evaluates these two aspects separately and generally utilizes standard engines (Sutisna & Ramadhan, 2025; Sugiarto et al., 2025; Fayisa et al., 2025). Comparative studies linking performance, fuel consumption, and noise across different exhaust configurations remain limited (Sutisna & Ramadhan, 2025), particularly when the cylinder capacity has been increased through a bore-up. This gap is significant because an increase in cylinder capacity alters the discharge and characteristics of the exhaust flow compared to standard conditions (Sutisna & Ramadhan, 2025; Duc et al., 2021). This study responds to this gap by simultaneously evaluating three alternative configurations—namely standard, free-flow, and High Performance Low Pollution Muffler (HPLPM) Mod 2 exhausts—on a 145 cm³ bore-up Yamaha Jupiter Z engine (Sutisna & Ramadhan, 2025; Uzoechi et al., 2025). The four outputs—torque, power, fuel consumption, and noise level—are analyzed as a single performance package to map the engineering trade-offs among the configurations (Sutisna & Ramadhan, 2025; Huang et al., 2025). This approach positions exhaust variations as alternative design solutions that can be compared based on the intended application, rather than in a simple dichotomy of "good" and "bad" configurations.

The scientific contribution of this research lies in presenting multi-criteria experimental evidence on a single bore-up engine. Unlike studies that separate performance and acoustic evaluations (Sugiarto et al., 2025; Fayisa et al., 2025), this research integrates torque, power, fuel consumption, and noise levels to present a more comprehensive pattern of engineering trade-offs (Sutisna & Ramadhan, 2025; Ao et al., 2025). Its added value is not the claim that one configuration is always superior, but rather the provision of a decision-making basis for exhaust system design development that needs to balance performance, fuel efficiency, and noise control according to the application goals (Murali et al., 2021; Fu et al., 2025). Based on this gap, this study aims to experimentally evaluate the characteristics of standard, free-flow, and HPLPM Mod 2 exhausts concerning torque, power, fuel consumption, and noise levels on a 145 cm³ bore-up Yamaha Jupiter Z engine. The study also aims to explain the relationship patterns among parameters by referring to previously reported exhaust flow and gas exchange mechanisms (Uzoechi et al., 2025; Khoa & Lim, 2021). The primary focus is to determine the technical compromises of each configuration under identical testing conditions.

The working hypothesis of the study posits that differences in exhaust configurations will be followed by measurable differences in torque, power, fuel consumption, and noise levels, as each configuration creates distinct exhaust flow conditions. The mechanistic interpretation refers to the previously reported relationships between gas exchange, volumetric efficiency, and engine performance (Uzoechi et al., 2025; Khoa & Lim, 2021), as well as the relationship between muffler structure and acoustic characteristics (Huang et al., 2025; Ao et al., 2025). Due to a limited number of replications, this hypothesis is evaluated in a descriptive-comparative manner and is not treated as inferential significance testing. In this study, creativity is positioned at the level of engineering problem-solving: generating and evaluating alternative technical configurations based on measurable trade-offs. This framework enables the experimental results to serve not only as a comparison of exhaust performance but also as a basis for design iteration when performance, efficiency, and noise objectives must be simultaneously met.

## METHOD

This study employed a laboratory experimental method with a single-factor design to evaluate the effect of various exhaust configurations on torque, power, fuel consumption, and noise level characteristics in a 145 $cm^3$ bore-up Yamaha Jupiter Z engine (Sutisna & Ramadhan, 2025; Sugiarto et al., 2025). All tests were conducted under identical operating conditions so that changes in each parameter could be attributed to the exhaust configuration variations as the treatment variables. The independent variables in this study consisted of the exhaust configurations: standard, free-flow, and High-Performance Low Pollution Muffler (HPLPM) Mod 2. The dependent variables included torque, power, fuel consumption, and noise level. All other variables, including engine specifications, fuel type, ignition system, lubricant, tire pressure, operator, and testing procedures, were kept constant to minimize the influence of external factors on the test results (Choe et al., 2021; Pechout et al., 2022).

The four observed parameters encompassed engine torque, power, fuel consumption, and noise level. Torque and power were measured using a chassis dynamometer, fuel consumption was determined via the volumetric method, while noise levels were measured using an A-weighted sound level meter (Choe et al., 2021; Sugiarto et al., 2025; Pechout et al., 2022). Each test was conducted repeatedly, and the results were expressed as average values. Torque and power measurements were performed three times each, whereas fuel consumption and noise levels were each measured twice under every testing condition. The number of replications for each parameter was determined by considering the testing characteristics, the availability of laboratory facility time, and the consistency of experimental procedures, ensuring that all exhaust configurations were tested under identical conditions (Sugiarto et al., 2025). The measurement results were subsequently utilized as the basis for analysis in accordance with the data processing procedures described in Subchapter 2.7.

**Table 1.** Classification of Research Variables

| Variable Category | Description |
|---|---|
| Independent variable | Exhaust configurations (standard, free-flow, HPLPM Mod 2) |
| Dependent variables | Torque (N·m), Power (HP), Fuel Consumption (mL/min), Noise level (dB(A)) |
| Controlled variables | 145 $cm^3$ bore-up Yamaha Jupiter Z engine, fuel type, lubricant, tire pressure, transmission ratio, environmental testing conditions, operator, measuring instruments, testing procedures |
| Experimental method | Laboratory-based experimental investigation |
| Data collection | Chassis dynamometer, fuel volume measurement, sound level meter |

The test engine utilized was a four-stroke, single-cylinder, air-cooled Yamaha Jupiter Z featuring an SOHC valve mechanism and a spark-ignition (SI) system. This engine was selected because it possesses a representative configuration for small-displacement motorcycle modification research and is widely employed as a research object in studies concerning engine performance enhancement (Sutisna & Ramadhan, 2025; Sugiarto et al., 2025). All basic engine specifications are presented in Table 2.

**Table 2.** Technical Specifications of the Test Engine

| Parameter | Specification |
|---|---|
| Engine model | Yamaha Jupiter Z |
| Engine type | Four-stroke, single-cylinder |
| Cooling system | Air-cooled |
| Valve mechanism | SOHC |
| Fuel | Pertalite |
| Ignition system | CDI (standard configuration) |
| Transmission | Manual, constant mesh |

Engine modification was performed by increasing the piston diameter (bore) to 58.5 mm while maintaining a piston stroke of 54 mm, thereby increasing the cylinder displacement to approximately 145 cm³. The engine was also equipped with a camshaft featuring a valve lift of 8 mm for both intake and exhaust valves, with opening durations of 110° and 100°, respectively. This modification configuration was applied to yield an increased cylinder displacement capable of influencing exhaust gas flow characteristics and engine performance, as reported in studies concerning spark-ignition engine modifications (Uzoechi et al., 2025; Khoa & Lim, 2021). Throughout the experiments, all components except the exhaust system were maintained constant, making the exhaust configuration the sole treatment variable (Sugiarto et al., 2025).

**Table 3.** Engine Modification Specifications

| Parameter | Value |
|---|---|
| Piston diameter (bore) (mm) | 58.5 |
| Stroke (mm) | 54 |
| Cylinder capacity (cm³) | 145 |
| Intake valve lift (mm) | 8 |
| Exhaust valve lift (mm) | 8 |
| Intake valve duration (°) | 110 |
| Exhaust valve duration (°) | 100 |

This study evaluated three exhaust configurations: standard, free-flow, and High Performance Low Pollution Muffler (HPLPM) Mod 2. These three were selected because they represent distinct exhaust gas flow resistance characteristics, as reported in various studies concerning exhaust systems and muffler designs (Sutisna & Ramadhan, 2025; Murali et al., 2021; Ao et al., 2025). All configurations were tested using the same engine specifications, fuel, operating conditions, and testing procedures so that result variations could be attributed to the characteristics of each respective exhaust (Sugiarto et al., 2025). The utilized exhaust configurations:

(a) (b) (c)

**Figure 1.** Exhausts (a) Standard, (b) Free-flow, (c) HPLPM Mod 2

The three exhaust configurations used in this study possessed differing physical specifications, as presented in Figure 1. The standard exhaust featured a total length of 350 mm, an inlet diameter of 20 mm, an outlet diameter of 20 mm, a weight of 2,200 g, and was made of iron. The free-flow exhaust featured a total length of 460 mm, an inlet diameter of 51 mm, an outlet diameter of 49 mm, a weight of 1,280 g, and was made of stainless steel. The High Performance Low Pollution Muffler (HPLPM) Mod 2 exhaust featured a total length of 340 mm, an inlet diameter of 51 mm, an outlet diameter of 10 mm, a weight of 1,330 g, and was made of stainless steel. All configurations were installed alternately on the same test engine under identical operating conditions, fuel, and testing procedures, ensuring that the exhaust configuration variation remained the sole treatment variable in this study.

**Table 4.** Configuration Characteristics

| Configuration | Design Characteristics |
|---|---|
| Standard exhaust | Manufacturer configuration with built-in damping system. |
| Free-flow exhaust | Exhaust gas channel with lower flow resistance. |
| HPLPM Mod 2 exhaust | Modified internal flow path configuration and damping system. |

All instruments were calibrated prior to testing to minimize measurement errors and enhance the reliability of experimental data (Choe et al., 2021; Pechout et al., 2022). The equipment utilized included a SPORTDYNO V3.3 chassis dynamometer, a 10 mL burette, a digital stopwatch, an A-weighted sound level meter, and a digital tachometer. Figure 2 displays the equipment configuration utilized for power and torque testing. Measurements were conducted using a chassis dynamometer connected to SPORTDYNO V3.3 software, while engine rotational speed was monitored in real-time using a digital tachometer (Choe et al., 2021).

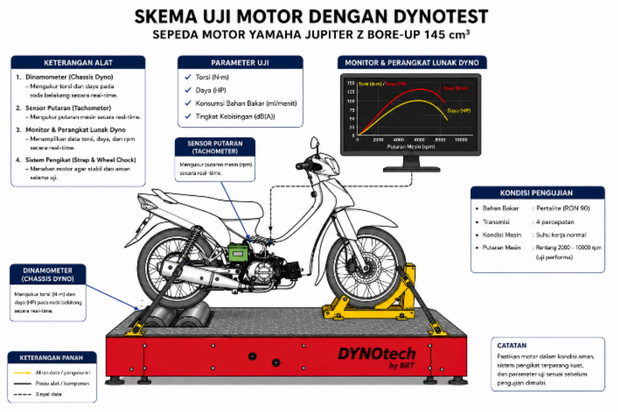


**Figure 2.** Schematic of power and torque testing.

During performance measurements, the motorcycle was tested using a SPORTDYNO V3.3 chassis dynamometer operating under the inertia method. The inertia method was chosen because it effectively characterizes two-wheeled vehicle performance via dynamometer roller acceleration and has been widely applied in motorcycle performance testing (Choe et al., 2021; Sugiarto et al., 2025; Pechout et al., 2022). Testing data were recorded automatically by the SPORTDYNO V3.3 software during the testing process. Each exhaust configuration was tested three times, and measurement results were expressed as average values (Sugiarto et al., 2025).

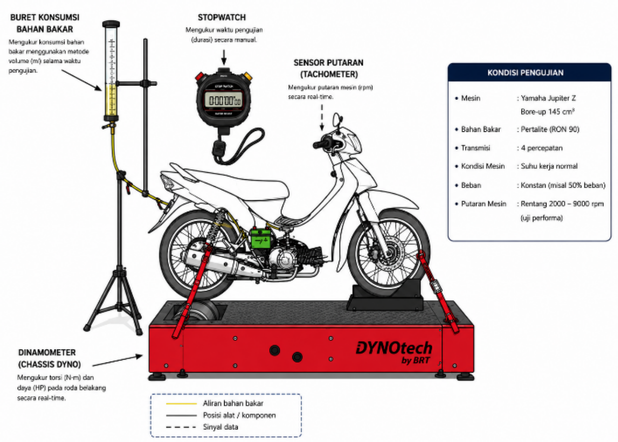


**Figure 3.** Schematic of fuel consumption testing

Fuel consumption was measured using a volumetric method with a 10 mL capacity burette (Pechout et al., 2022; Duy et al., 2021). The time required for the engine to consume this fuel volume was recorded using a digital stopwatch; subsequently, the fuel consumption rate was calculated based on the ratio between the fuel volume and the measurement time (Duc et al., 2021). Testing was performed twice at each engine speed (2,000, 4,000, and 6,000 rpm), and the results were expressed as average values.

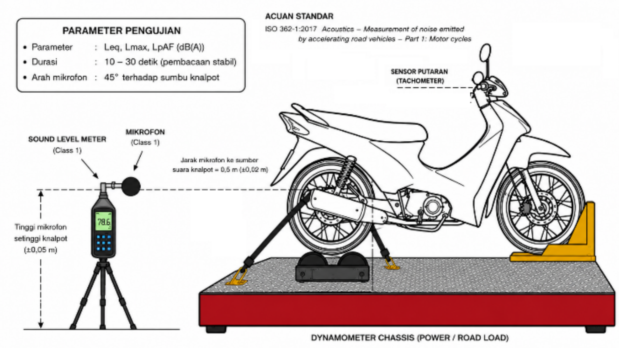


**Figure 4.** Schematic of noise level measurement

Noise levels were measured using an A-weighted sound level meter [dB(A)] positioned at a fixed location, distance, and orientation relative to the exhaust tip (Sutisna & Ramadhan, 2025; Fayisa et al., 2025). Testing was performed twice at each engine speed, and the results were expressed as average values to enable direct comparisons among exhaust configurations. Engine rotational speed was monitored using a digital tachometer throughout all testing to ensure that every measurement was executed at the predetermined engine speed (Sugiarto et al., 2025). A digital stopwatch was utilized to record the time required for fuel consumption measurements and to maintain identical sampling durations during each experimental condition (Uzoechi et al., 2025; Pechout et al., 2022).

**Table 5.** Testing Instruments Used

| Instrument | Specification | Function |
|---|---|---|
| Chassis Dynamometer | SPORTDYNO V3.3, inertia method | Measuring torque and power |
| Measuring cylinder/burette | 10 mL measurement volume | Measuring fuel consumption via volumetric method |
| Digital stopwatch | Digital time measurement | Measuring fuel consumption time |
| Sound Level Meter | A-weighting [dB(A)] | Measuring exhaust noise level |
| Digital Tachometer | Engine speed reading range (rpm) | Monitoring engine speed during testing |

Prior to testing, the motorcycle was mounted on the chassis dynamometer, the designated exhaust configuration was installed, and the engine was warmed up until reaching a stable operating temperature to ensure all tests were conducted under uniform operating conditions (Choe et al., 2021; Pechout et al., 2022). Each exhaust configuration was tested according to the established number of repetitions to enhance measurement repeatability (Sugiarto et al., 2025). Mean and standard deviation values were subsequently calculated for all data to serve as the basis for comparative analysis among exhaust configurations (Murali et al., 2021).

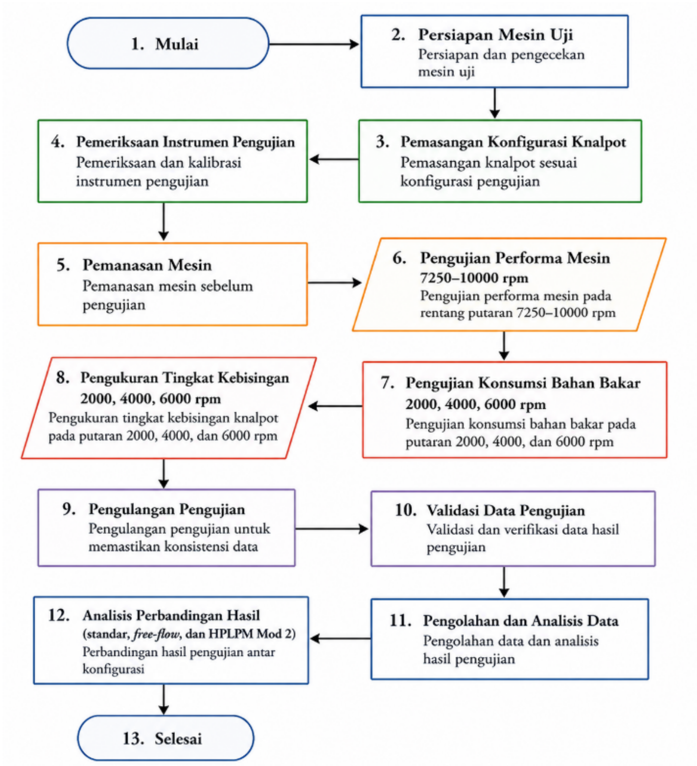


**Figure 5.** Flowchart of the Experimental Testing Procedure

Test data were processed to obtain torque, power, fuel consumption, and noise level parameters as the foundation for comparative analysis across exhaust configurations (Choe et al., 2021; Pechout et al., 2022). Engine torque was acquired directly from the chassis dynamometer data acquisition system. The measured torque represents the effective rotational force transmitted to the drive wheels through the entire drivetrain (Sugiarto et al., 2025). Torque is expressed in Newton-meters (N·m) and serves as a primary indicator of engine output. Power was calculated based on torque and engine speed values obtained from chassis dynamometer testing (Sugiarto et al., 2025). The relationship among power, torque, and engine speed is expressed in Equation (1):

$$P = \frac{2\pi NT}{60000} \quad \dots\dots\dots (1)$$

The power value obtained from Equation (1) was subsequently converted into horsepower (HP) units using a conversion factor of 1 kW = 1.341 HP (Equation 2) to align with the output units of the SPORTDYNO V3.3 software:

$$P_{HP} = 1.341 \times P_{kW} \quad \dots\dots\dots (2)$$

Fuel consumption was determined using the volumetric method (Duc et al., 2021; Pechout et al., 2022). During each test, 10 mL of fuel was supplied to the engine while the time required to consume this fuel was recorded using a digital stopwatch. The volumetric fuel consumption rate was calculated using Equation (3):

$$FC = \frac{V}{T} \quad \dots\dots\dots (3)$$

The noise level of each exhaust configuration was evaluated using a sound level meter. Measurement results were expressed in A-weighted decibels [dB(A)] and utilized as a basis for comparing acoustic characteristics among exhaust configurations (Deshmukh et al., 2025; Fayisa et al., 2025). Mean values were utilized to obtain representative figures for each test parameter and were calculated using Equation (4):

$$\bar{x} = \frac{\sum_{i=1}^{n} x_i}{n} \quad \dots\dots\dots (4)$$

The repeatability of experimental measurements was evaluated using the standard deviation calculated via Equation (5):

$$SD = \sqrt{\frac{\sum_{i=1}^{n}(x_i - \bar{x})^2}{n-1}} \quad \dots\dots\dots (5)$$

Measurement uncertainty was controlled through the utilization of calibrated instruments, uniform testing procedures, and the management of research variables as detailed in Subchapter 2.1 (Pechout et al., 2022; Sugiarto et al., 2025).

**Table 7.** Data Processing Methods

| Parameter | Measurement Source | Measurement Method |
|---|---|---|
| Torque, $T$ (N·m) | Chassis dynamometer | Direct measurement |
| Power, $P$ (HP) | Torque and engine speed | Equation (1) |
| Fuel consumption ($mL/min$) | Volumetric method | Equation (3) |
| Noise level ($dB(A)$) | Sound level meter | Direct measurement |
| Mean value | Repeated measurements | Arithmetic mean |
| Standard deviation | Repeated measurements | Statistical calculation |

**Table 8.** Statistical Analysis Procedures

| Analysis Level | Method | Objective |
|---|---|---|
| Test replication | Replication according to research design | Enhance result repeatability of tests |
| Mean calculation | Arithmetic mean | Determine representative value for each test parameter |
| Standard deviation calculation | Standard deviation | Ascertain data spread and consistency levels |
| Result analysis | Comparative descriptive analysis | Evaluate the effect of exhaust variations on torque, power, fuel consumption, and noise levels |

Test data were analyzed descriptively by comparing torque, power, fuel consumption, and noise level values across exhaust configurations, adhering to the analytical approach commonly applied in experimental engine performance research (Choe et al., 2021; Gabana et al., 2025). Measurement outcomes were presented in tables and graphs to illustrate response trends for each parameter against exhaust configuration variations. Given the relatively limited number of test replications ($n = 2$ for fuel consumption and noise levels, and $n = 3$ for torque and power), this study did not perform inferential statistical significance tests such as one-way ANOVA or nonparametric tests. Consequently, result interpretation focused on comparing mean values, standard deviations, pattern consistencies across exhaust configurations, and their alignment with mechanisms reported in previous studies (Sutisna & Ramadhan, 2025; Pechout et al., 2022). This approach was selected to prevent drawing potentially unreliable statistical conclusions arising from restricted sample sizes. Subsequent result interpretation was performed by linking performance parameter trends and acoustic characteristics to exhaust flow theory while comparing them with prior findings (Sutisna & Ramadhan, 2025; Murali et al., 2021; Khoa & Lim, 2021).

Data reliability was maintained by repeating measurements for each exhaust configuration under identical operating conditions (Sugiarto et al., 2025; Pechout et al., 2022). Result consistency was evaluated using mean and standard deviation values, whereas measurement validity was supported by utilizing calibrated instruments and uniform testing protocols across all exhaust configurations (Choe et al., 2021; Gabana et al., 2025). Nevertheless, the limited number of test replications constitutes a research limitation, directing the obtained results more toward illustrating response trends for each exhaust configuration rather than making statistical generalizations to a broader population. The validity of mechanistic interpretations is constrained by available parameters. This study did not directly measure backpressure, exhaust gas temperature, air-fuel ratio (AFR), brake specific fuel consumption (BSFC), volumetric efficiency, or emissions (Sutisna & Ramadhan, 2025; Murali et al., 2021; Pechout et al., 2022). Therefore, these parameters were not utilized as causal evidence but rather as a theoretical context to interpret the measured torque, power, fuel consumption, and noise characteristics. Consequently, the primary conclusions of the study are restricted to empirical comparisons among exhaust configurations. Direct measurements of backpressure, exhaust gas temperature, AFR, BSFC, and emissions are required in future studies to examine the underlying mechanisms governing performance changes, fuel efficiency, and acoustic characteristics (Sutisna & Ramadhan, 2025; Murali et al., 2021; Ao et al., 2025). This limitation is crucial to ensure that interpretations do not exceed the capabilities of the experimental design employed.

## RESULTS AND DISCUSSION

Engine performance characteristics were evaluated based on torque and power obtained through testing using a chassis dynamometer across an engine speed range of 7,250–10,000 rpm (Choe et al., 2021; Gabana et al., 2025). Both parameters were analyzed simultaneously as they represent the engine's capability to generate twisting force and effective power as a consequence of changes in exhaust gas flow characteristics due to exhaust configuration variations (Duc et al., 2021; Pechout et al., 2022). The relatively small standard deviation values for each parameter indicate that the test results possessed good repeatability, rendering the obtained data sufficiently consistent to be used as a basis for comparative analysis (Sugiarto et al., 2025).

Descriptively, the free-flow configuration produced higher torque and power compared to both the standard exhaust and the HPLPM Mod 2 across nearly the entire engine speed range. Conversely, the HPLPM Mod 2 tended to produce lower performance outputs but exhibited more stable curve changes. This pattern demonstrates differences in performance characteristics among configurations that are consistent with the role of the exhaust system in shaping flow conditions and gas exchange (Sutisna & Ramadhan, 2025; Murali et al., 2021; Sugiarto et al., 2025). Because inferential analysis was not performed, these differences were not interpreted as statistically "significant."

**Table 9.** Torque and power test results for each exhaust configuration (mean ± SD, n = 3)

| Engine Speed (rpm) | Torque, T (N·m) | | | Power, P (HP) | | |
|---|---|---|---|---|---|---|
| | Standard | Free-flow | HPLPM Mod 2 | Standard | Free-flow | HPLPM Mod 2 |
| 7250 | 8.60 ± 1.04 | 9.63 ± 0.88 | 8.66 ± 0.34 | 8.83 ± 1.06 | 9.87 ± 0.93 | 8.87 ± 0.38 |
| 7500 | 10.00 ± 0.66 | 10.16 ± 0.36 | 9.35 ± 0.52 | 10.60 ± 0.69 | 10.77 ± 0.35 | 9.90 ± 0.53 |
| 7750 | 10.26 ± 0.23 | 10.37 ± 0.37 | 9.05 ± 0.47 | 11.23 ± 0.25 | 11.37 ± 0.40 | 9.93 ± 0.47 |
| 8000 | 9.81 ± 0.13 | 10.05 ± 0.28 | 8.31 ± 0.27 | 11.10 ± 0.17 | 11.33 ± 0.29 | 9.40 ± 0.26 |
| 8250 | 9.22 ± 0.14 | 9.88 ± 0.19 | 7.50 ± 0.38 | 10.73 ± 0.15 | 11.50 ± 0.20 | 8.77 ± 0.47 |
| 8500 | 8.81 ± 0.30 | 9.74 ± 0.18 | 7.09 ± 0.42 | 10.60 ± 0.36 | 11.70 ± 0.17 | 8.57 ± 0.51 |
| 8750 | 8.56 ± 0.10 | 9.91 ± 0.11 | 7.21 ± 0.16 | 10.60 ± 0.10 | 11.93 ± 0.67 | 8.93 ± 0.21 |
| 9000 | 8.46 ± 0.14 | 9.86 ± 0.09 | 7.17 ± 0.23 | 10.77 ± 0.15 | 12.23 ± 0.64 | 9.13 ± 0.29 |
| 9250 | 8.23 ± 0.07 | 9.88 ± 0.17 | 7.11 ± 0.33 | 10.80 ± 0.10 | 12.90 ± 0.20 | 9.30 ± 0.44 |
| 9500 | 7.80 ± 0.11 | 9.75 ± 0.15 | 6.69 ± 0.37 | 10.53 ± 0.15 | 13.10 ± 0.20 | 8.97 ± 0.49 |
| 9750 | 7.28 ± 0.19 | 9.42 ± 0.04 | 6.21 ± 0.21 | 10.07 ± 0.25 | 13.03 ± 0.06 | 8.57 ± 0.23 |
| 10000 | 6.28 ± 0.13 | 9.11 ± 0.04 | 5.65 ± 0.14 | 8.90 ± 0.20 | 12.90 ± 0.10 | 7.97 ± 0.21 |

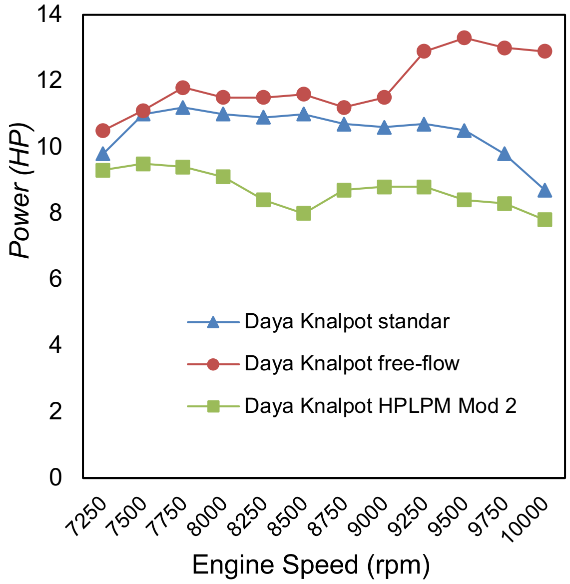


**Figure 6.** Graph of Power

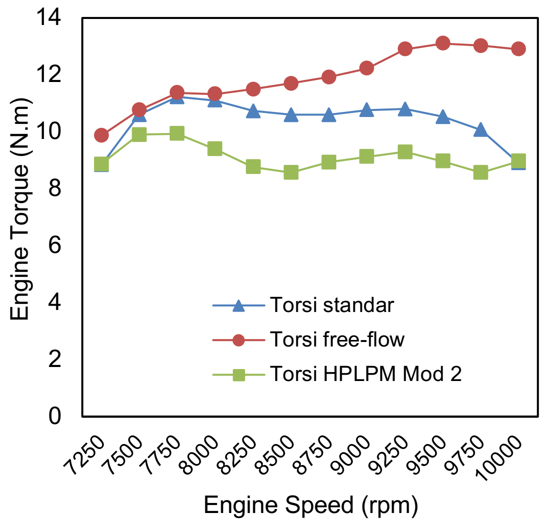


**Figure 7.** Graph of Torque

The data in Table 9, as well as Figure 6 and Figure 7, demonstrate that exhaust configuration variations produced distinct performance characteristics across the entire engine speed range. The performance characteristic differences observed among the three exhaust configurations indicate alterations in the exhaust gas flow mechanisms. Although parameters such as backpressure, the gas exchange process, and volumetric efficiency were not measured directly in this study, these changes are suspected to contribute to the differences in torque and power outputs, as elucidated in various previous studies (Sutisna & Ramadhan, 2025; Murali et al., 2021; Khoa & Lim, 2021).

The free-flow configuration generated the highest torque and power across almost the entire engine speed range. Mechanistically, this pattern is consistent with the probable reduction in exhaust gas flow resistance and the increased effectiveness of combustion residual gas discharge, as discussed in the literature concerning backpressure and engine performance (Sutisna & Ramadhan, 2025; Pechout et al., 2022; Duy et al., 2021). However, backpressure was not directly measured in this study; therefore, this mechanism is treated as a theoretically supported interpretation, rather than a cause-and-effect relationship proven by pressure measurement data. The maximum torque in the free-flow configuration increased by approximately 16.7% compared to the standard exhaust. The magnitude of this difference indicates that the output characteristics of a bore-up engine can be sensitive to the exhaust system configuration (Sutisna & Ramadhan, 2025; Khoa & Lim, 2021; Yimer & Nallamothu, 2025). At a 145 cm³ capacity, a larger exhaust flow discharge can theoretically magnify the consequences of flow path modifications; nevertheless, this interpretation remains descriptive because the study did not directly measure backpressure, volumetric efficiency, or flow parameters.

The findings of this study demonstrate trends consistent with various prior studies reporting that reducing backpressure can enhance volumetric efficiency through a more effective gas exchange process. In this study, this mechanism was not directly observed, but the obtained pattern of torque increase indicates the likelihood of a similar process occurring. Therefore, the performance improvement in the free-flow configuration is interpreted as a trend consistent with mechanisms reported in the literature (Novella et al., 2024; Sutisna & Ramadhan, 2025; Murali et al., 2021; Khoa & Lim, 2021), rather than direct evidence regarding changes in backpressure or volumetric efficiency.

The magnitude of this improvement is a specific characteristic of the 145 cm³ bore-up Yamaha Jupiter Z engine with the testing configuration employed in this study. Thus, direct comparisons with other studies should be made cautiously because differences in engine capacity, modification specifications, fuel systems, operating conditions, and testing procedures can yield different performance responses (Yimer & Nallamothu, 2025; Shaik et al., 2025). The tendency for performance improvement in configurations with lower flow resistance aligns with mechanisms discussed in earlier studies (Sutisna & Ramadhan, 2025; Huang et al., 2025; Wang et al., 2023). However, the magnitude of the improvement in this study cannot be attributed to a single factor. The bore-up engine condition, camshaft specifications, ignition system, and the geometric characteristics of each exhaust provide a context that limits the generalization of the results. Therefore, the findings are primarily utilized to compare alternative configurations on the same test engine.

The increase in torque in the free-flow configuration was followed by an increase in power since both parameters possess a mathematical relationship to engine speed. Maximum power reached 13.10 HP, representing an increase of approximately 21.3% compared to the standard exhaust and 40.9% compared to the HPLPM Mod 2. This pattern indicates that the reduction in exhaust gas flow resistance likely correlates with a more effective discharge process of combustion residual gases at high engine speeds. Nonetheless, because neither backpressure nor volumetric efficiency parameters were directly measured, this mechanism is viewed as an interpretation supported by theory and prior research. The standard exhaust produced relatively lower performance compared to the free-flow configuration but exhibited more uniform output characteristics across the entire engine speed range. This condition reflects the manufacturer's exhaust design philosophy, which prioritizes a balance among performance, riding comfort, noise levels, and operational reliability over the attainment of maximum power (Sutisna & Ramadhan, 2025; Murali et al., 2021).

The HPLPM Mod 2 generated lower torque and power compared to the free-flow configuration but exhibited better performance curve stability. This condition indicates that the internal configuration of the HPLPM Mod 2 likely provides different exhaust flow characteristics compared to the free-flow configuration. This difference is suspected to be related to the pressure wave attenuation mechanism and an increase in exhaust flow resistance, as explained in previous studies (Ao et al., 2025; Fu et al., 2025; Walle et al., 2025). Despite this, the mechanism was not verified through direct measurements, thus this interpretation should be understood as a theoretical explanation supporting the experimental results.

The differences in performance characteristics obtained across the three exhaust configurations demonstrate that exhaust system optimization is not solely determined by the ability to lower backpressure. The internal geometric design of the exhaust also influences pressure wave propagation, the scavenging process, as well as pumping losses during the exhaust stroke (Sutisna & Ramadhan, 2025; Kepekçi & Ağca, 2024; Kreß et al., 2024). Overall, the research results signify that exhaust system optimization cannot be based solely on efforts to reduce exhaust flow resistance. The internal geometric design of the exhaust needs to consider the balance among gas flow characteristics, pressure wave propagation, and acoustic attenuation capabilities (Huang et al., 2025; Ao et al., 2025; Fu et al., 2025). In this study, the free-flow configuration provided the highest performance, whereas the HPLPM Mod 2 offered a better compromise between performance enhancement and noise level control, meaning that the selection of the exhaust configuration needs to be tailored to the vehicle's intended application.

From an engineering creativity perspective, the three configurations exhibit three distinct design priorities. The free-flow maximized performance output, the HPLPM Mod 2 steered the design toward a performance-acoustic compromise, while the standard exhaust maintained more conservative characteristics. These findings reaffirm that technically relevant design creativity is not synonymous with pursuing a single maximum value; the quality of a solution is determined by the configuration's suitability to the intended goals and operational limits to be fulfilled. Fuel consumption testing was conducted to evaluate the effect of exhaust configuration variations on fuel use efficiency at engine speeds of 2,000, 4,000, and 6,000 rpm (Yang et al., 2024; Rosdi et al., 2025). This parameter was analyzed to identify the relationship between exhaust gas flow characteristics and fuel requirements across various engine operating conditions (Sutisna & Ramadhan, 2025; Pechout et al., 2022).

**Table 10.** Fuel consumption test results for each exhaust configuration (mean ± SD, n = 2)

| **Engine Speed (rpm)** | **Fuel Consumption (mL/min)** | | |
|---|---|---|---|
| | **Standard** | **Free-flow** | **HPLPM Mod 2** |
| 2000 | 8.69 ± 0.14 | 7.51 ± 0.04 | 7.69 ± 0.06 |
| 4000 | 21.73 ± 3.07 | 12.98 ± 6.36 | 20.83 ± 0.00 |
| 6000 | 30.30 ± 0.62 | 32.25 ± 0.70 | 31.25 ± 0.00 |

The mean and standard deviation values in Table 10 indicate that variations in the measurement results were relatively small, rendering the data suitable for comparing fuel consumption characteristics across exhaust configurations. Generally, the free-flow configuration exhibited the lowest fuel consumption at low to medium engine speeds, while at high engine speeds, fuel consumption increased compared to the other configurations. Conversely, the standard exhaust and HPLPM Mod 2 displayed more moderate changes in fuel consumption across the entire engine speed range. These findings indicate that changes in exhaust gas flow characteristics affect fuel requirements according to engine operating conditions. Quantitatively, this trend indicates that changes in exhaust configurations not only affect the magnitude of fuel consumption but also alter the consumption pattern at each engine speed range. Therefore, the subsequent discussion focuses on the mechanisms causing differences in fuel consumption characteristics among exhaust configurations.

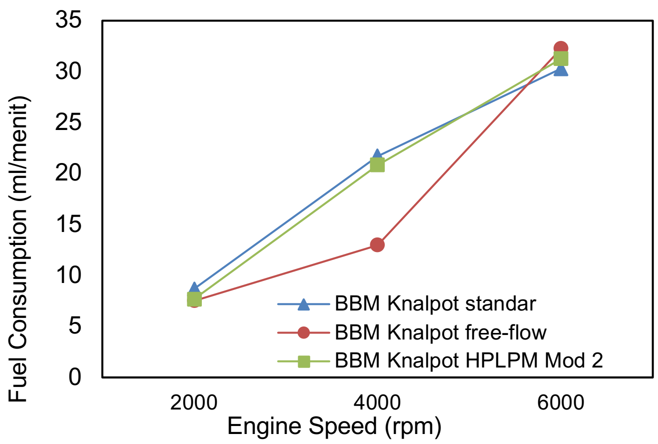


**Figure 8.** Graph of Fuel Consumption

Based on Table 10 and Figure 8, the three configurations exhibited different fuel consumption patterns at each engine speed. These data demonstrate that changes in exhaust configurations correlate with changes in fuel requirements under identical operating conditions. Because the air-fuel ratio, volumetric efficiency, and backpressure were not directly measured, the mechanism linking the exhaust configuration with fuel consumption was not established causally in this study. The free-flow configuration exhibited the lowest fuel consumption at low to medium engine speeds. This pattern is consistent with the likely occurrence of a more effective gas exchange process under those conditions, as discussed regarding trends in engine consumption and performance studies (Yang et al., 2024; Rosdi et al., 2025). However, this result does not imply that a reduction in flow resistance has been directly proven to cause a reduction in fuel consumption, because flow parameters and mixture composition were not measured. At low to medium engine speeds, the fuel consumption advantage in the free-flow configuration appeared alongside a performance enhancement. This pattern is consistent with the more effective gas exchange mechanisms discussed in the literature (Sutisna & Ramadhan, 2025; Khoa & Lim, 2021). Simultaneously, the relationship between performance and fuel requirements remains dependent on engine operating conditions and mixture formation strategies (Novella et al., 2024; Duy et al., 2021). Thus, the research results are more appropriately read as an inter-configuration response map rather than as singular evidence regarding combustion mechanisms.

Nevertheless, at 6000 rpm, the differences in fuel consumption among configurations diminished. This condition indicates that the increased demand for the air-fuel mixture at high engine speeds offset the efficiency advantages gained by the free-flow configuration at low to medium engine speeds. Thus, fuel use efficiency is influenced not only by the characteristics of the exhaust system but also by the increased load and engine energy requirements at high engine speeds. This phenomenon demonstrates that the influence of the exhaust configuration on fuel use efficiency tends to decrease as engine energy requirements increase (Shaik et al., 2025; Wang et al., 2023).

This phenomenon implies that the engine performance enhancement generated by the free-flow configuration at high engine speeds necessitated a larger supply of air-fuel mixture to sustain the combustion process. In other words, the increase in power and torque in this configuration was followed by an increase in fuel consumption at higher operating conditions. Thus, the performance enhancement obtained was not an absolute consequence of energy efficiency improvement, but rather the result of an increased supply of chemical energy via greater fuel consumption (Novella et al., 2024; Rosdi et al., 2025). Conversely, the standard and HPLPM Mod 2 configurations exhibited more stable fuel consumption characteristics, although they did not generate performance as high as the free-flow configuration. Overall, the research results demonstrate that the relationship between engine performance and fuel consumption is one of engineering trade-offs (Sutisna & Ramadhan, 2025; Murali et al., 2021; Huang et al., 2025). The free-flow configuration provided advantages in the form of both performance enhancement and fuel use efficiency at low to medium engine speeds. However, at high engine speeds, this performance enhancement was accompanied by an increase in fuel consumption as a consequence of elevated combustion energy requirements. Conversely, the standard and HPLPM Mod 2 configurations yielded more stable fuel consumption characteristics, even though they were incapable of producing performance as high as the free-flow configuration. Therefore, the selection of the exhaust configuration needs to be tailored to the vehicle's usage characteristics so that an optimal balance between performance and fuel use efficiency can be achieved (Ao et al., 2025; Fu et al., 2025). Noise levels were evaluated to determine the capability of each exhaust configuration in attenuating the acoustic energy generated during the combustion residual gas discharge process (Ao et al., 2025; Walle et al., 2025). The analysis was conducted under identical operating conditions so that differences in noise levels could be directly associated with the internal characteristics of the exhaust system (Deshmukh et al., 2025). Measurements were conducted using an A-weighted sound level meter [dB(A)] at engine speeds of 2000, 4000, and 6000 rpm (Deshmukh et al., 2025; Fayisa et al., 2025). All tests were performed with the same instrument positioning, environmental conditions, and procedures so that measurement results could be compared directly across exhaust configurations (Pechout et al., 2022). Each test was conducted twice, and the mean value was calculated as the basis for analysis.

**Table 11.** Noise level test results for each exhaust configuration (mean ± SD, n = 2)

| Engine Speed (rpm) | Noise Level (dBA) | | |
|---|---|---|---|
| | Standard | Free-flow | HPLPM Mod 2 |
| 2000 | 82.55 ± 2.05 | 88.20 ± 2.83 | 82.35 ± 0.35 |
| 4000 | 90.50 ± 0.28 | 98.80 ± 0.28 | 87.15 ± 0.78 |
| 6000 | 96.30 ± 0.71 | 101.85 ± 1.34 | 95.55 ± 0.35 |

The relatively small standard deviation values indicate that the measurement results possessed good repeatability, rendering the data suitable for use as a basis for comparative analysis among exhaust configurations (Sugiarto et al., 2025). The test results exhibited a consistent pattern: the HPLPM Mod 2 produced the lowest noise levels across all testing conditions, whereas the free-flow produced the highest noise levels. This descriptive difference aligns with the principle that internal geometry and muffler damping elements influence acoustic attenuation capabilities (Ao et al., 2025; Fu et al., 2025; Walle et al., 2025). Because the study did not perform inferential significance testing, the term "significant" is not utilized to denote differences among configurations.

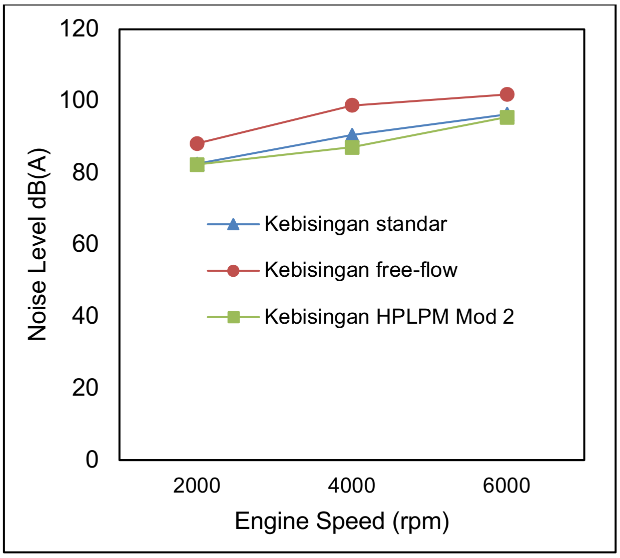


**Figure 9.** Graph of Noise Levels

Based on the test results, the noise levels of all exhaust configurations increased as engine speed escalated. At 2000 rpm, the standard exhaust configuration produced a noise level of 82.6 dB(A), while the free-flow exhaust reached 88.2 dB(A) and the HPLPM Mod 2 was 82.4 dB(A). A similar increase occurred at 4000 rpm, which was 90.5 dB(A) for the standard exhaust, 98.8 dB(A) for the free-flow, and 87.2 dB(A) for the HPLPM Mod 2. At 6000 rpm, noise levels further increased to 96.3 dB(A) for the standard exhaust, 101.9 dB(A) for the free-flow, and 95.6 dB(A) for the HPLPM Mod 2. These results demonstrate that the free-flow configuration consistently produced the highest noise levels, whereas the HPLPM Mod 2 provided the lowest noise levels across most testing conditions (Sugiarto et al., 2025; Murali et al., 2021).

The free-flow configuration generated the highest torque and power. This increase is suspected to be related to the exhaust gas flow characteristics possessing lower resistance compared to the other configurations, facilitating a potentially more effective combustion residual gas discharge process. This interpretation is consistent with theory and prior research concerning the effect of backpressure on engine performance (Sutisna & Ramadhan, 2025; Pechout et al., 2022). Quantitatively, the maximum noise level of the free-flow exhaust reached 101.85 dB(A), whereas the standard exhaust produced 96.30 dB(A) and the HPLPM Mod 2 produced 95.55 dB(A). Thus, the free-flow configuration increased the noise level by approximately 5.8% compared to the standard exhaust and about 6.6% compared to the HPLPM Mod 2. Conversely, the HPLPM Mod 2 was able to reduce the noise level by approximately 6.2% compared to the free-flow configuration, demonstrating the effectiveness of the internal damping system in reducing acoustic energy without eliminating the engine's overall performance characteristics (Ao et al., 2025; Fu et al., 2025; Walle et al., 2025).

Conversely, the HPLPM Mod 2 produced lower noise levels compared to both the standard and free-flow exhausts. This characteristic signifies that the internal design of the HPLPM Mod 2 was capable of attenuating pressure wave propagation more effectively through a combination of expansion chambers, flow direction changes, and damping elements within the muffler (Ao et al., 2025; Walle et al., 2025). This mechanism reduces acoustic energy intensity before the exhaust gas is released into the environment, resulting in lower noise levels (Deshmukh et al., 2025; Ao et al., 2025). The HPLPM Mod 2 produced lower noise but also lower torque and power compared to the free-flow. This pattern is consistent with the presence of a compromise between the acoustic attenuation function and the freedom of exhaust gas flow (Sutisna & Ramadhan, 2025; Murali et al., 2021; Huang et al., 2025). Because pressure loss and backpressure were not directly measured, this study does not conclude that increased flow resistance was the measurable cause; this mechanism is utilized as a theoretical explanation that still requires verification through subsequent measurements.

These results are consistent with prior studies indicating that expansion chambers, perforated pipes, and sound-absorbing materials increase transmission loss, thereby lowering noise levels (Ao et al., 2025; Fu et al., 2025; Walle et al., 2025). However, this improvement in damping capability is generally accompanied by an increase in pressure loss, rendering engine performance enhancements more limited (Sutisna & Ramadhan, 2025; Kreß et al., 2024). Overall, the HPLPM Mod 2 configuration provided the best acoustic characteristics, whereas the free-flow configuration provided the highest engine performance with the consequence of increased noise levels. These results reaffirm that exhaust system design must consider the balance among performance requirements, fuel use efficiency, and noise level control in accordance with the vehicle's application goals (Sugiarto et al., 2025; Huang et al., 2025; Ao et al., 2025).

In an integrated manner, the research results demonstrate that changes in exhaust configurations were followed by changes in torque, power, fuel consumption, and noise levels. The literature concerning backpressure and gas exchange provides a plausible mechanistic explanation for these patterns (Sutisna & Ramadhan, 2025; Murali et al., 2021; Khoa & Lim, 2021; Pechout et al., 2022), but the data in this study primarily support comparative, rather than causal, conclusions. The most crucial finding is that no single configuration dominated all criteria: the free-flow excelled in performance, whereas the HPLPM Mod 2 excelled in noise control and offered a more balanced compromise. Within the framework of engineering creativity, this pattern forms a "design space" that can be utilized to select or develop subsequent configurations based on application priorities.

This study possessed several limitations that constrain generalizability and mechanistic interpretation. Testing was conducted on a single 145 $cm^3$ bore-up Yamaha Jupiter Z engine, using one fuel type, and three exhaust configurations; thus, the responses on engines with different capacities, valve timing, or fuel systems cannot yet be ascertained (Novella et al., 2024; Sutisna & Ramadhan, 2025; Duc et al., 2021). Furthermore, the number of replications was limited, and the study did not measure backpressure, exhaust gas temperature, air-fuel ratio (AFR), brake specific fuel consumption (BSFC), volumetric efficiency, or emissions. Therefore, cause-and-effect relationships between exhaust geometry and performance changes still require more comprehensive experimental verification.

Future research needs to combine performance measurements with backpressure, AFR, exhaust gas temperature, BSFC, emissions, and acoustic characteristics so that mechanisms of change can be tested directly. Design development can also be directed toward evaluating internal geometry, expansion chambers, perforation channels, and wave propagation characteristics to seek Pareto configurations that balance performance and noise (Huang et al., 2025; Ao et al., 2025; Kepekçi & Ağca, 2024; Kreß et al., 2024). With a larger number of replications, inferential statistical analysis or multi-objective optimization can be employed to assess solution stability and strengthen the foundation for design selection. Within the engineering creativity framework, this study demonstrates that the value of a design alternative lies in its ability to resolve inter-criteria conflicts, rather than merely enhancing a single parameter. The characteristic differences among the standard, free-flow, and HPLPM Mod 2 exhausts are consistent with the principle that the exhaust system configuration plays a role in shaping the balance of performance, fuel use efficiency, and acoustic characteristics (Sutisna & Ramadhan, 2025; Murali et al., 2021; Uzoechi et al., 2025; Ao et al., 2025). Thus, the contribution of this research is to provide experimental evidence that can serve as a basis for design evaluation and iteration in the development of bore-up engine exhaust systems.

## CONCLUSION

This study descriptively demonstrates that three exhaust configurations yielded distinct technical compromises on a 145 $cm^3$ bore-up Yamaha Jupiter Z engine. The free-flow configuration provided the highest performance, with a maximum torque of 13.10 N·m and a maximum power of 13.10 HP, as well as lower fuel consumption at low to medium engine speeds, but this consumption advantage did not persist at high engine speeds. The HPLPM Mod 2 provided the best acoustic control, with a maximum noise level of 95.55 dB(A), lower than the free-flow which reached 101.85 dB(A), indicating that this configuration offers a more balanced compromise when noise becomes a design constraint. The absence of a single configuration excelling in all parameters reaffirms that exhaust selection is a multi-objective engineering problem. The research contribution to engineering creativity lies in utilizing multi-criteria evidence to evaluate design alternatives based on application goals, rather than solely on maximum power output. The conclusions are limited by a relatively small number of replications and the absence of direct measurements of backpressure, AFR, BSFC, exhaust gas temperature, volumetric efficiency, and emissions; therefore, the causal mechanisms for the changes still require verification in subsequent studies utilizing more comprehensive measurements and optimization.

## REFERENCES


Ao, S., Yang, H., Liu, Y., Jin, M., Su, H., Ma, Y., ... Xue, J. (2025). Design and Testing of a Gasoline Engine Muffler Based on the Principle of Split-Stream Rushing. *Applied Sciences, 15*(3), 1078.

Choe, T. H., Ryu, Z. R., Kang, S. G., & Ri, J. P. (2021). Mathematical Modeling of the Two-Stroke Crankcase Scavenged Spark Ignition Engine Working Process. *Energy Conversion and Management: X, 10*, 100086.

Deshmukh, N. N., Mane, K. V., Nadar, J., Pereira, R., Shelar, R., & David, R. (2025). Experimental and Simulation Study to Evaluate Effect of Radial Air Injection on Performance of Motorcycle Silencers. *Journal of Thermal Engineering, 11*(3), 703–715.

Duc, K. N., Nguyen, Y. L. T., Duy, T. N., Nghiem, T. D., Le, A. T., & Huu, T. P. (2021). A Robust Method for Collecting and Processing the On-Road Instantaneous Data of Fuel Consumption and Speed for Motorcycles. *Journal of the Air & Waste Management Association, 71*(1), 81–101.

Duy, V. N., Duc, K. N., & Van, N. C. (2021). Real-Time Driving Cycle Measurements of Fuel Consumption and Pollutant Emissions of a Bi-Fuel LPG-Gasoline Motorcycle. *Energy Conversion and Management: X, 12*, 100135.

Fayisa, F., Roziqin, A., Naryanto, R. F., Septiyanto, A., Maulana, S., & Rohman, S. (2025). Analisis Pengujian Konsumsi Bahan Bakar dan Performa pada Sepeda Motor Honda 110 cc Menggunakan Knalpot AHLM (Adaptive High-Performance, Low-Pollution Muffler). *Panthera: Jurnal Ilmiah Pendidikan Sains dan Terapan, 5*(4), 1228–1239.

Fu, J., Cheng, M., Ma, Y., & Zheng, W. (2025). Investigation on the Influence of Airflow on the Acoustic Performance of a Single–Cylinder Diesel Engine Exhaust Muffler. *PLoS ONE, 20*(6), e0318210.

Gabana, P., Gimenez, B., Herreros, J. M., & Tsolakis, A. (2025). Analysis of the Combustion Speed in a Spark Ignition Engine Fuelled With Hydrogen and Gasoline Blends at Different Air Fuel Ratios. *Fuel, 381*, 133563.

Huang, P., Wu, P., Su, H., Xue, J., Zhang, H., Zhang, Y., & Guo, Y. (2025). Research on the Acoustic Attenuation Performance and Optimization of Split-Stream Rushing Exhaust Mufflers in the Presence of Acoustic–Structure Coupling Effects. *Applied Sciences, 15*(9), 4722.

Iurk, M. A., Och, S. H., Moura, L. M., Mariani, V. C., & Domingues, E. (2021). Maximizing Volumetric Efficiency Using Stochastic Optimization Techniques for Internal Combustion Engines. *Applied Thermal Engineering, 199*, 117603.

Kepekçi, H., & Ağca, M. E. (2024). Numerical Investigation of the Thermal and Acoustic Effect of Material Variations on the Exhaust Muffler. *International Journal of Automotive Engineering and Technologies, 13*(1), 33–44.

Khoa, N. X., & Lim, O. (2021). A Study to Investigate the Effect of Valve Mechanisms on Exhaust Residual Gas and Effective Release Energy of a Motorcycle Engine. *Energies, 14*(17), 5564.

Kreß, J., Rau, J., Behr, I., Mohn, B., Hebert, H., & Morgado-Estévez, A. (2024). Exhaust Gas Improvement of Modern Scooters by Velocity Control. *Control Engineering Practice, 153*, 106111.

Markiewicz, M. (2024). Analysis of Performance Parameters of Engines With Spark Ignition With Variable Regulations of the Fuel-Injection System, Powered by E100 Fuel. *Energies, 17*(3), 601.

Murali, R., Shahriman, A. B., Razlan, Z. M., Ahmad, W. K. W., Azizul, A. I., Rojan, M. A., ... Ibrahim, Z. (2021). A Review on the Correlation Between Exhaust Backpressure and the Performance of IC Engine. *Journal of Physics: Conference Series, 2051*(1), 012044.

Novella, R., Gomez-Soriano, J., González-Domínguez, D., & Olaciregui, O. (2024). Optimizing Hydrogen Spark-Ignition Engine Performance and Pollutants by Combining VVT and EGR Strategies Through Numerical Simulation. *Applied Energy, 376*, 124307.

Pechout, M., Jindra, P., Hart, J., & Vojtisek-Lom, M. (2022). Regulated and Unregulated Emissions and Exhaust Flow Measurement of Four In-Use High Performance Motorcycles. *Atmospheric Environment: X, 14*, 100170.

Pirrello, D., Teodosio, L., & Berni, F. (2024). 1D Model and Rule-Based Calibration Strategy to Improve the Performance of a Turbocharged Spark Ignition Engine Over the Whole Engine Map. *Engineering Science and Technology, an International Journal, 60*, 101890.

Rosdi, S. M., Ghazali, M. F., & Mamat, R. (2025). Evaluation of Engine Performance and Emissions Using Blends of Gasoline, Ethanol, and Fusel Oil. *Case Studies in Chemical and Environmental Engineering, 11*, 101065.

Shaik, F., Kumar, D. V., Naik, N. C. K., Krishna, G. R., Khan, T Y., Shaik, A. S., ... Emma, A. F. (2025). Predictive Modeling and Optimization of SI Engine Performance and Emissions With GEM Blends Using ANN and RSM. *Scientific Reports, 15*(1), 4585.

Sugiarto, M., Herdiyatno, Y. D., Prasetyo, H., Karyanto, Y., Sadili, R., & Hardianto, D. (2025). Air Optimization on Motorcycle Intake Manifold Towards Work Performance and Exhaust Gas Emissions. *Jurnal Teknologi Transportasi dan Logistik, 6*(1), 85–94.

Sutisna, N. A., & Ramadhan, I. A. (2025). Comparative Analysis of Noise, Emission, and Performance of Shijiro Racing Exhaust With Standard Exhaust on a 2020 Vespa Sprint 150 I-Get. *ROTASI, 27*(2), 49–63.

Uzoechi, S. G., Ezechukwu, V. C., & Swift, O. N. K. (2025). Examining the Thermal Performance of a Muffler in a Spark Ignition Engine. *IPS Journal of Engineering and Technology, 1*(3), 128–135.

Wang, P., Duan, X., Chen, C., & Liu, S. (2023). Experimental Investigation on the Exhaust Emissions and Performance of a Hybrid Electric Motor Coupled With an Energy Recovery System. *Case Studies in Thermal Engineering, 45*, 102994.

Walle, M., Yeneneh, K., & Sufe, G. (2025). Investigation of Spark Ignition Engine Performance in Ethanol–Petrol Blended Fuels Using Artificial Neural Network. *Scientific Reports, 15*(1), 25516.

Yang, L., Jia, X., Liao, X., Zhang, J., & Chu, Z. (2024). Study on Sporty Exhaust Sound of Economical Vehicle Under Acceleration. *Journal of Low Frequency Noise, Vibration and Active Control, 43*(4), 1517–1529.

Yimer, A. M., & Nallamothu, R. B. (2025). Reduction of the Noise From the Engine, Modification of Reactive Muffler and Performance Analysis. *Discover Applied Sciences, 7*(8), 849.